

The Type VI secretion system deploys anti-fungal effectors against microbial competitors

Katharina Trunk¹, Julien Peltier^{2,4}, Yi-Chia Liu¹, Brian D. Dill², Louise Walker⁶, Neil A.R. Gow⁶, Michael J.R. Stark³, Janet Quinn⁴, Henrik Strahl⁵, Matthias Trost^{2,4*} and Sarah J. Coulthurst^{1*}

¹Division of Molecular Microbiology, ²MRC Protein Phosphorylation and Ubiquitylation Unit, ³Centre for Gene Regulation and Expression, School of Life Sciences, University of Dundee, Dow St, Dundee, DD1 5EH, UK; ⁴Institute for Cell and Molecular Biosciences, Newcastle University, Framlington Place, Newcastle-upon-Tyne, NE2 4HH, UK; ⁵Centre for Bacterial Cell Biology, Newcastle University, Richardson Road, Newcastle-upon-Tyne, NE2 4AX, UK; ⁶Aberdeen Fungal Group, Institute of Medical Sciences, MRC Centre for Medical Mycology at the University of Aberdeen, Foresterhill, Aberdeen, AB25 2ZD, UK.

*Correspondence may be addressed to Sarah Coulthurst (s.j.coulthurst@dundee.ac.uk) or Matthias Trost (matthias.trost@newcastle.ac.uk)

1 **Interactions between bacterial and fungal cells shape many polymicrobial communities.**
2 **Bacteria elaborate diverse strategies to interact and compete with other organisms, including**
3 **the deployment of protein secretion systems. The Type VI secretion system (T6SS) delivers toxic**
4 **effector proteins into host eukaryotic cells and competitor bacterial cells. Yet surprisingly,**
5 **T6SS-delivered effectors targeting fungal cells have not been reported. Here we show that the**
6 **‘anti-bacterial’ T6SS of *Serratia marcescens* can act against fungal cells, including pathogenic**
7 ***Candida* species, and identify the novel effector proteins responsible. These first anti-fungal**
8 **effectors, Tfe1 and Tfe2, have distinct and species-specific impacts on the target cell, but both**
9 **can ultimately cause fungal cell death. ‘In competition’ proteomics analysis revealed that T6SS-**
10 **mediated delivery of Tfe2 disrupts nutrient uptake and amino acid metabolism in fungal cells,**
11 **and leads to the induction of autophagy. Intoxication by Tfe1, in contrast, causes a loss of**
12 **plasma membrane potential. Our findings extend the repertoire of the T6SS and suggest that**
13 **anti-fungal T6SSs represent widespread and important determinants of the outcome of**
14 **bacterial-fungal interactions.**

15
16 Bacteria and fungi frequently cohabit in a multitude of different environments, from abiotic
17 surroundings, such as soil, to plant and mammalian hosts, including polymicrobial infection sites.
18 Bacteria may develop strategies to profit from the metabolic activity of neighbouring fungal cells, for
19 example utilising fungal breakdown products from otherwise inaccessible organic material.
20 Conversely, they may elaborate antagonistic strategies to contain growth of competing microbes, such
21 as efficient scavenging of scarce nutrients or direct attack upon the competitor^{1,2}. Gram-negative
22 bacteria utilise complex transport machineries, protein secretion systems, to translocate effector
23 proteins into other cells³. Following translocation, the bacterial effector destroys or reprogrammes the
24 target cell for the benefit of the secreting bacterium. The Type VI secretion system (T6SS) is a
25 widespread, bacteriophage-like machinery that fires toxic effectors into neighbouring cells. It uses a
26 tubular contractile sheath to expel a cell-puncturing structure, decorated with a variety of effector
27 proteins, out of the bacterial cell towards the target⁴⁻⁶. Some of these effectors are deployed against

1 higher eukaryotes, representing classical anti-host virulence factors⁷. Nevertheless, recent findings
2 indicate that the function of most T6SSs is to deliver anti-bacterial toxins into rival bacterial cells,
3 providing a competitive advantage in mixed bacterial populations. These T6SS-delivered anti-
4 bacterial effectors, including toxins targeting the bacterial cell wall, cell membrane and nucleic acids,
5 are each associated with a specific immunity protein to protect the secreting cell and its siblings from
6 self-intoxication^{8,9}. Surprisingly, however, given the close association of bacteria and fungi in many
7 environments, no anti-fungal effectors delivered by the T6SS have been reported to date.

8

9 **Results**

10 **The anti-bacterial T6SS of *Serratia marcescens* displays anti-fungal activity**

11 To investigate whether the bacterial T6SS could affect proliferation of eukaryotic microorganisms
12 commonly encountered in microbial communities, the ubiquitous yeast *Saccharomyces cerevisiae* was
13 used as a model target organism. *Serratia marcescens* Db10, which possesses a well-characterised and
14 potent anti-bacterial T6SS¹⁰, was utilised as the bacterial ‘attacker’. Co-culture of these two organisms
15 resulted in >100-fold decrease of recovered viable yeast cells, indicating that *S. marcescens*, itself a
16 ubiquitous microorganism, can restrict fungal proliferation in mixed microbial cultures (Fig. 1a).
17 When co-cultures were performed using *S. marcescens* $\Delta tssE$, a T6SS-inactive mutant, recovery of
18 viable fungal cells was unaffected, demonstrating that the observed inhibition is T6SS-dependent
19 (Fig. 1a). Direct translocation of effector proteins into a target cell requires the T6SS to puncture and
20 traverse the target cell wall. Considering the thickness and rigidity of the fungal cell wall¹¹ and that
21 the *S. marcescens* T6SS readily releases secreted proteins to the extracellular medium¹², we
22 considered that anti-fungal toxins might instead be secreted into the external milieu with subsequent
23 uptake by the fungal cell. When the assay was repeated with bacterial and fungal cells separated by a
24 cell-impermeable membrane, the number of recovered fungal cells was independent of the T6SS
25 functionality of the underlying bacterial strain and comparable to that when placed directly on the
26 media (Fig. 1a). Thus bacterial-fungal cell contact is essential for anti-fungal T6SS activity. Next, the
27 range of fungal target cells was expanded to include pathogenic fungi, namely *Candida* species,
28 clinically-important fungal pathogens commonly residing with bacteria in polymicrobial infection

1 sites^{2, 13}. We tested *Candida albicans*, the most frequently-isolated fungal pathogen in humans, and
2 the phylogenetically-distant *Candida glabrata*, which displays intrinsic resistance to common anti-
3 fungal drugs¹⁴. Both organisms were susceptible to T6SS-mediated anti-fungal activity, indicating a
4 broad anti-fungal action of the *S. marcescens* T6SS (Fig. 1b).

5

6 **Identification of two anti-fungal T6SS effector proteins**

7 Having established fungi as a new target kingdom of the *S. marcescens* T6SS, we sought to identify
8 the effector proteins responsible. The potential anti-fungal activity of six previously-identified T6SS-
9 secreted proteins (Ssp1-6¹²) was tested by utilising specific effector deletion mutants as attacker
10 strains. Deletion of *SMDB11_1112* (*ssp3*) resulted in a 4-fold increase in recovery of viable *C.*
11 *albicans* target cells compared with the wild type, although it had little effect on *S. cerevisiae* or *C.*
12 *glabrata* (Fig. 1c). *SMDB11_1112* was therefore renamed Tfe1 (T6SS anti-fungal effector 1).

13 Subsequent deletion of five more effectors (mutant Δ *sspI-6*) had no additional effect on the survival
14 of fungal cells (Supplementary Fig. 1), suggesting the existence of further, unidentified T6SS-
15 dependent effector(s).

16 To identify additional potential effectors, we employed a cellular proteomics approach, a
17 complementary strategy to our previous secretome analysis, with the rationale that T6SS-secreted
18 proteins would be retained inside the cell of a T6SS-inactive mutant. Using label-free quantitative
19 mass spectrometry, we quantified 3034 proteins, representing 64% of the *S. marcescens* Db10
20 genome. Twelve proteins were identified as having significantly increased intracellular abundance in
21 the Δ *tssE* mutant compared with the wild type (Fig. 2a, Supplementary Data 1, Supplementary Fig. 2).
22 Nine were known secreted components or effectors of the T6SS machinery^{12, 15}, including Tfe1,
23 validating the approach. The remaining three proteins, of unknown functions, represented new T6SS-
24 secreted effector candidates. Since, as a predicted lipoprotein, *SMDB11_1031* is unlikely to be
25 available for T6SS-dependent secretion, we focused on the two remaining candidates, *SMDB11_1083*
26 and *SMDB11_3457*, the latter encoded downstream of two Hcp homologues. Neither candidate is
27 encoded adjacent to potential cognate immunity proteins (Fig. 2b). This non-compliance with one of
28 the main criteria for anti-bacterial effectors⁸ further marked them as potential anti-fungal agents.

1 To determine whether SMDB11_1083 or SMDB11_3457 are T6SS-delivered anti-fungal toxins, the
2 respective deletion mutants were used as attacking strains in bacterial-fungal co-cultures. Whereas
3 loss of SMDB11_3457 did not have any effect on anti-fungal activity of *S. marcescens*, removal of
4 SMDB11_1083 resulted in almost complete loss of activity against *S. cerevisiae* or *C. glabrata* and
5 reduced activity against *C. albicans* (Fig. 1c). SMDB11_1083 therefore represents a second T6SS-
6 delivered anti-fungal effector, named Tfe2. When *C. albicans* was co-cultured with a mutant lacking
7 Tfe1 and Tfe2, the partial anti-fungal activity seen with either single mutant was eliminated.
8 Expression of Tfe1 and Tfe2 *in trans* was able to restore fungal inhibition in the respective deletion
9 mutants (Fig. 1d). Overexpression of Tfe1 decreased anti-fungal activity against *S. cerevisiae* and *C.*
10 *glabrata*, perhaps indicating that competition between Tfe1 and Tfe2 for the T6SS machinery resulted
11 in reduced delivery of the more potent Tfe2. Finally, confirming that Tfe1 and Tfe2 are not required
12 for T6SS function, mutants lacking Tfe1 and Tfe2 had no impairment in their ability to secrete the
13 expelled component Hcp or the effector Ssp2 (Fig. 1e), or in anti-bacterial activity against
14 *Pseudomonas fluorescens* (Supplementary Fig. 3).

15 Tfe1 can induce mild growth inhibition if overexpressed in bacterial cells, which is alleviated by co-
16 expression with the immunity protein Sip3¹². However, in contrast to mutants lacking immunity
17 proteins for true anti-bacterial effectors^{12, 15, 16}, the $\Delta sip3$ mutant is fully fit and is not sensitive to the
18 T6SS of the wild type or a Tfe1-overexpressing strain (Supplementary Fig. 3). These data suggest that
19 the intended target of Tfe1 is not bacterial cells, but that Sip3 acts as a failsafe against non-specific
20 toxicity should excess Tfe1 occur. For Tfe2, no anti-bacterial toxicity could be detected upon
21 overexpression nor candidate immunity gene identified. Additionally, the *S. marcescens* T6SS, and by
22 implication its effectors, does not appear to act against higher eukaryotic organisms, since T6SS-
23 inactive mutants show no loss of virulence in several models (ref¹⁷, Supplementary Fig. 4). Taken
24 together, we conclude that Tfe1 and Tfe2 are the major anti-fungal toxins deployed by the T6SS of *S.*
25 *marcescens* and are likely to be used only against fungal cells.

26

27 **Tfe1 and Tfe2 exhibit distinct and target-specific anti-fungal activity**

28 Bioinformatic analysis failed to reveal conserved domains or predicted functions for Tfe1 or Tfe2.

1 Therefore their impact on fungal cell integrity was investigated following growth in co-culture with *S.*
2 *marcescens*. With *C. albicans* as the target, cell distortion and lysis was detected, dependent on the
3 T6SS and Tfe1 in the attacking bacteria (Fig. 3a). Consistently, many necrotic *C. albicans* cells were
4 observed by cryo-TEM following co-culture with wild type *S. marcescens*, whereas few such cells
5 were seen with a T6SS-inactive mutant (Supplementary Fig. 5). With *S. cerevisiae* or *C. glabrata*,
6 granular structures were observed in a T6SS- and Tfe2-dependent manner (Fig. 3a), consistent with
7 the primary role of Tfe2 against both organisms in co-culture viability assays (Fig. 1). Propidium
8 iodide (PI) stains cells which have lost the membrane permeability barrier, a common indirect proxy
9 for loss of viability. We observed that ~50% of *C. albicans* and *C. glabrata* cells recovered from co-
10 cultures with *S. marcescens* showed PI-staining, dependent on the T6SS and either Tfe1 (*C. albicans*)
11 or Tfe2 (*C. glabrata*) (Fig. 3b). These observations are consistent with co-culture viable count assays
12 (Fig. 1), where recovery of viable fungal cells co-cultured with wild type *S. marcescens* was lower
13 than the initial inoculum, implying fungicidal action. In contrast, PI-staining was not observed in *S.*
14 *cerevisiae*. To confirm directly that Tfe1 and Tfe2 possess intrinsic anti-fungal activity, and
15 investigate further their impact on the different fungal species, each effector was expressed in *S.*
16 *cerevisiae* and *C. albicans* using galactose- and doxycycline-inducible¹⁸ expression systems,
17 respectively. Expression of Tfe1, but not the anti-bacterial effectors Ssp1 and Ssp2, strongly inhibited
18 growth of *S. cerevisiae* and induced abnormally large vacuoles and cell lysis (Fig. 3d,e;
19 Supplementary Fig. 6), confirming the fungicidal potential of Tfe1. Similarly, expression of Tfe1 in
20 *C. albicans* caused growth inhibition and cell death (Supplementary Fig. 7) and reproduced the Tfe1-
21 dependent morphological changes observed in co-culture (Fig.3c). Expression of Tfe2 in *S.*
22 *cerevisiae*, whilst not causing obvious changes in morphology, was able to abolish growth, even at
23 very low levels (Fig. 3c,d).
24 Induction of Tfe2 during logarithmic growth of *S. cerevisiae* in liquid cultures resulted in a decline in
25 the number of viable cells over time, whilst cell density approached steady-state. Upon removal of
26 induction, yeast cells recovered from Tfe2-induced growth inhibition within 3 h to resume normal
27 growth (Fig. 4a). These results indicate that Tfe2-mediated intoxication of *S. cerevisiae* primarily
28 results in growth inhibition, with reduced long-term survival as a downstream consequence. To

1 investigate whether the fungistatic effect of Tfe2 on *S. cerevisiae* was caused by inhibition of
2 metabolic activity, the fluorescent dye FUN1 was utilised. Metabolically-active cells transport the dye
3 into the vacuole where it forms distinct tubular structures which exhibit red fluorescence. In
4 metabolically-inactive cells, the dye remains in the cytoplasm and fluoresces green¹⁹. Bright red
5 structures, apparently vacuole-associated and similar to those observed in the control strain, were
6 detected during early stages of Tfe1 expression when the cells gained dramatically in size (Fig. 4b),
7 eventually being replaced by green fluorescence before onset of lysis. Tfe2-expressing cells also
8 displayed bright red fluorescent structures, however, these appeared more globular, dispersed and
9 mainly outside the vacuole. Together with the persistence of green fluorescence, this indicates that
10 Tfe2 causes reduced cellular metabolic activity and potential interference with vacuolar transport²⁰.
11 To determine whether either effector causes loss of plasma membrane potential, *S. cerevisiae* cells
12 expressing Tfe1 or Tfe2 were stained with the voltage-dependent dye DiBAC₄(3) which enters cells in
13 a depolarisation-dependent manner. Tfe1 intoxication resulted in membrane depolarisation, similar to
14 treatment with mellitin and amphotericin B, whereas Tfe2 caused no loss of membrane potential (Fig.
15 4c). Co-staining with PI revealed that only a fraction of the Tfe1-intoxicated cells showing
16 depolarisation also exhibited a loss of membrane integrity, in contrast with the action of the pore-
17 forming peptide mellitin where all depolarised cells were also permeabilised (Fig. 4d, Supplementary
18 Fig. 8). Intoxication of *C. albicans* by T6SS-delivered Tfe1 caused a similar pattern of membrane
19 depolarisation and selective permeability (Supplementary Fig. 9). Thus our data suggest that Tfe1
20 primarily causes a loss of membrane potential, which is not due to pore formation but can ultimately
21 lead to a loss of membrane integrity, and imply that Tfe1 and Tfe2 act on different cellular targets in
22 fungal cells.

23

24 **The T6SS can act on filamentous fungal cells**

25 Whilst *P. aeruginosa* has been reported to preferentially kill the hyphal form of *C. albicans*²¹, we had
26 so far demonstrated T6SS activity against the budding yeast form. Co-culture of *S. marcescens* with
27 the constitutively filamentous *tup1Δ* mutant²² revealed PI-staining of individual cell segments within
28 filaments, with this localised action being dependent on the T6SS and Tfe1 (Fig. 4e,f). A T6SS- and

1 Tfe1-dependent drop in viable cell counts was also observed (Supplementary Fig. 10). Thus the anti-
2 fungal *S. marcescens* T6SS can intoxicate budding and filamentous forms of *C. albicans*.

3

4 **‘In competition’ proteomics reveals that T6SS-delivered Tfe2 disrupts nutrient transport and** 5 **metabolism and induces autophagy**

6 To identify specific cellular pathways affected by the anti-fungal effectors in a physiologically-
7 relevant context, namely when delivered by the T6SS, we performed ‘in competition’ proteomics
8 using *C. albicans* as target. Fungal cells were co-cultured with wild type *S. marcescens* Db10, the
9 T6SS-inactive mutant $\Delta tssE$, or effector mutants, $\Delta tfe1$, $\Delta tfe2$ and $\Delta tfe1\Delta tfe2$, before performing
10 quantitative mass spectrometric analysis of the total fungal proteome in each condition using isotope-
11 labelled tandem mass tags (six-plex TMT). 4446 *C. albicans* proteins (~72% of the genome) and 2486
12 *S. marcescens* proteins were quantified (Supplementary Data 2, Supplementary Fig. 11-15). Of the *C.*
13 *albicans* proteins, 1667 showed significant modulation across the five-way comparison (ANOVA-
14 positive, $p < 0.05$). Hierarchical clustering of these modulated proteins confirmed that Tfe1 and Tfe2
15 cause disruption of different fungal pathways. The analysis also demonstrated that the major response
16 of *C. albicans* is to T6SS-dependent translocation of Tfe2, since the response to the $\Delta tfe2$ mutant was
17 similar to that of $\Delta tssE$ or $\Delta tfe1\Delta tfe2$ (Fig. 5a). To identify individual proteins within this set as being
18 robustly altered in specific response to Tfe2, we further imposed requirements for a significant change
19 in abundance (>1.3 -fold) to be observed in the presence of the wild type compared with the $\Delta tfe2$
20 mutant, and for a consistent change to be observed in $\Delta tfe1\Delta tfe2$ and $\Delta tssE$ mutants. According to
21 these criteria, 14 fungal proteins were upregulated in response to Tfe2 delivery and 16 downregulated
22 (Supplementary Table 1). In contrast, no Tfe1-specific proteins were identified using these strict
23 criteria. This may, at least in part, reflect Tfe1 acting on a non-protein target, consistent with its ability
24 to induce plasma membrane depolarisation. Evaluation of the 30 Tfe2-responsive proteins by Gene
25 Ontology enrichment analysis identified significant overrepresentation of proteins belonging to the
26 cellular amino acid biosynthetic process (GOID 8652), specifically arginine biosynthesis (GOID
27 6526) and sulfur amino acid biosynthesis (GOID 0097), as well as anion transport (GOID 6820) (Fig.
28 5b; see also Supplementary Fig. 16). Therefore subsequent analysis was focused on these areas of

1 nutrient uptake and amino acid metabolism.

2 Fungal cells must acquire sulfur from their environment for the *de novo* biosynthesis of cysteine,
3 methionine and other organic sulfur metabolites, such as glutathione²³. The sole sulfate transporter in
4 *C. albicans*, Sul2, and members of the sulfate assimilation pathway were strongly decreased in the
5 presence of Tfe2-translocating bacteria. Heat map analysis of relevant proteins revealed
6 downregulation of the entire pathway for reduction of inorganic sulfate to homocysteine in response
7 to Tfe2 (Fig. 5c). Similar to Sul2, two general amino acid permeases, Gap1 and Gap2, and two basic
8 amino acid permeases, Can1 and Can2, all of which transport arginine into the fungal cell²⁴⁻²⁶, were
9 subject to Tfe2-dependent downregulation (Fig. 5d). Furthermore, examination of arginine metabolic
10 proteins²⁷ in the proteomics dataset indicated Tfe2-dependent accumulation of proteins involved in
11 arginine synthesis, whereas proteins mediating arginine catabolism were unchanged or decreased (Fig.
12 5d). Consistent with this profile, intracellular arginine levels in *S. cerevisiae* expressing Tfe2 were
13 increased 4-fold compared with control cells (Fig. 6a). Lysine levels were also increased, and a
14 further 14 amino acids displayed a range of down- or upregulation, indicating extensive nutrient
15 imbalance upon Tfe2-mediated intoxication.

16 Next, we determined if Tfe2-induced reduction of fungal nutrient transporters, which also included
17 the peptide transporter Ptr22 (Supplemental Table 1), is due to transcriptional downregulation. Plasma
18 membrane transporter expression is induced by substrate, which is sensed by the transporter itself, as
19 for Sul2, or by non-transporting membrane proteins, including the amino acid sensor Csy1 (Ssy1 in *S.*
20 *cerevisiae*), a component of the SPS sensing complex^{28, 29}. Transcript levels of the sensor gene *SSY1*,
21 SPS-activated transcriptional regulators *STP1* and *STP2*, and SPS-controlled permease genes³⁰⁻³² were
22 increased upon expression of Tfe2 in *S. cerevisiae* (Fig. 6b). This implies that Tfe2 does not inhibit
23 SPS sensing or signalling. Rather, transcriptional induction of the SPS-regulon is consistent with
24 Tfe2-induced intracellular nutrient depletion or imbalance. Similarly, sulfate transporter transcript
25 levels were upregulated by Tfe2, despite downregulation at the protein level. We confirmed that
26 T6SS-mediated delivery of Tfe2 decreases levels of Can1 in *S. cerevisiae*, with redistribution from the
27 plasma membrane suggesting vacuolar degradation (Supplementary Fig. 17). These data indicate that
28 Tfe2 intoxication causes depletion of nutrient transporters at a post-transcriptional level. In turn, the

1 resulting decrease in intracellular nutrients may lead to downregulation of nutrient-utilisation
2 pathways, as observed for proteins of the sulfate assimilation pathway (Fig. 5c), or in upregulation of
3 compensatory metabolic pathways, as observed for arginine synthesis (Fig. 5d).
4 Further evidence for Tfe2-dependent interference with the intracellular amino acid pool was the
5 marked increase in the bZip transcriptional activator protein Gcn4 (Supplemental Table 1), which
6 mediates the general amino acid control (GAAC) response to amino acid starvation^{33, 34}. The
7 proteomics data also revealed a Tfe2-dependent increase in the levels of Atg1, a Ser/Thr kinase
8 subject to regulation by the nutrient-sensing TOR signalling pathway. Activation of Atg1 by
9 phosphorylation in response to nitrogen and amino acid starvation leads to induction of autophagy³⁵.
10 To investigate if Tfe2-mediated amino acid limitation leads to autophagy, we analysed proteolytic
11 processing of the autophagy reporter protein GFP-Atg8^{36, 37} in *S. cerevisiae* co-cultured with *S.*
12 *marcescens*. With yeast alone, only full length GFP-Atg8 was observed. Upon co-culture with wild
13 type *S. marcescens*, a band corresponding to free GFP was detected, indicating processing of GFP-
14 Atg8 by vacuolar peptidases and thus induction of autophagy. Processing was not detected upon co-
15 culture with bacteria lacking Tfe2 or a functional T6SS, nor in cells lacking the key autophagy
16 regulator, Atg13 (Fig. 6c, Supplementary Fig. 18). Hence induction of autophagy is dependent on
17 T6SS-mediated delivery of Tfe2. Although Tfe2 may induce autophagy independent of amino acid
18 imbalance, our results are consistent with the idea that Tfe2-mediated intoxication of fungal cells
19 leads to disruption of the intracellular amino acid pool, causing a starvation signal which induces
20 autophagy as a protective response.

21 Overall, we have revealed that Tfe2 intoxication leads to extensive nutrient imbalance, interference
22 with plasma membrane transporters and induction of autophagy. The precise aspect or combination of
23 these factors which ultimately leads to the death of the fungal cell remains to be deciphered. In
24 contrast, Tfe1 acts via a plasma membrane depolarising mechanism which does not involve formation
25 of large, unselective pores.

26

27 **Discussion**

28 Cellular proteomics combined with genetic analysis led us to discover the first T6SS-dependent anti-

1 fungal effectors, Tfe1 and Tfe2, whose T6SS-dependent secretion was confirmed in our concurrent
2 secretome study¹⁵. The two effectors elicit distinct responses in fungal cells and can exert a fungicidal
3 effect. The severity of the fungal response to each toxin differs between species, likely reflecting
4 divergence of metabolic pathways. ‘In competition’ proteomics revealed that T6SS-delivered Tfe2
5 disrupts fungal nutrient uptake and metabolism. In particular, Tfe2 intoxication strongly affected
6 inter-related pathways involved in sulfate assimilation, plasma membrane nutrient transport and
7 amino acid metabolism and also caused induction of autophagy. Autophagy is a process by which,
8 under nutrient-limiting stress conditions, fungal cells target cellular macromolecules for vacuolar
9 degradation and recycling^{35,38}. Induction of this pathway in response to Tfe2 indicates severe
10 disturbance of the intracellular metabolic equilibrium and may represent a protective response
11 attempting to rescue the viability of the fungal cell. A striking change in response to Tfe2 was
12 increased intracellular levels of arginine and lysine. Upregulation of arginine and lysine synthesis has
13 been linked to sudden nutrient limitation upon engulfment by neutrophils^{39,40}, and regulation of
14 arginine synthesis in response to phagocytosis may also represent a protective mechanism against the
15 phagocyte oxidative burst in *C. albicans*^{41,42}. Thus Tfe2 may be causing a similar response to that
16 induced upon phagocytosis. Tfe1, in contrast, does not provoke a strong proteomic response and
17 instead causes plasma membrane depolarisation, reminiscent of T6SS-delivered antibacterial effectors
18 which target the bacterial membrane⁸.

19 This study demonstrates that the bacterial T6SS can act as a potent anti-fungal weapon, causing
20 growth arrest and death of fungal cells. In agreement with the prevailing model, T6SS-dependent anti-
21 fungal activity required attacker-target cell-cell contact, suggesting that effector translocation occurs
22 directly into the fungal cell. Supporting the feasibility of this idea, cryo-TEM showed an intimate
23 interaction between cells of *C. albicans* and *S. marcescens* (Supplementary Fig. 5). Moreover, the
24 expelled arrow-like structure of the T6SS should have both the length (approximately 0.7 μm , at least
25 three times the thickness of the average fungal cell wall)⁴³⁻⁴⁵ and the force⁴ to puncture the rigid
26 fungal cell wall. The *S. marcescens* T6SS delivers multiple anti-bacterial effectors and is a potent
27 weapon against competitor bacteria^{15,17}. However this study reveals a second, prominent role for this
28 T6SS in controlling growth of co-habiting fungal micro-organisms. Whilst *Serratia-Candida*

1 interactions may on occasion be relevant clinically, given that both can colonise common sites such as
2 bloodstream, respiratory, and GI tracts^{2, 46, 47}, *Serratia* is ubiquitous in the environment and likely uses
3 its anti-fungal T6SS in diverse contexts. More importantly, our work implies that other bacterial
4 pathogens may deploy a T6SS against fungal cells during polymicrobial infection. This is supported
5 by the observation that Tfe2 homologues are present in other pathogenic T6SS-containing bacteria,
6 including *Pseudomonas* and *Vibrio* species. Thus, we propose that anti-fungal T6SS activity is
7 widespread and may be an intrinsic property of many, if not all, ‘anti-bacterial’ T6SSs. Indeed, one
8 report has suggested anti-yeast activity associated with a T6SS in *P. syringae*, although no effectors
9 were identified⁴⁸. The fact that T6SS anti-fungal effectors have not been discovered previously may
10 be partially attributable to many identification strategies relying on the presence of associated
11 immunity proteins, therefore excluding proteins such as Tfe2.

12 With the identification of a new class of effectors, anti-fungal toxins, we have expanded the repertoire
13 of the T6SS arsenal to include another target kingdom and highlighted another role for this versatile
14 machinery in shaping polymicrobial communities. Deployment of T6SSs enabling simultaneous
15 attack upon prokaryotic and fungal rivals should represent a key determinant of bacterial competitive
16 fitness in a multitude of environments, from rhizosphere to polymicrobial human infections.

1 **Methods**

2 **Bacterial strains, plasmids and culture conditions**

3 Bacterial strains and plasmids used in this study are given in Supplementary Table 2. Mutant strains
4 of *S. marcescens* Db10 carrying in-frame deletions were generated by allelic exchange using the
5 pKNG101 suicide vector, and effector genes were cloned into pSUPROM for constitutive expression
6 *in trans*¹⁰. To avoid non-specific anti-bacterial toxicity upon complementation of the $\Delta tfe1$ strain by
7 plasmid-encoded Tfe1, the cognate immunity gene *sip3* was included in the construct. All primer
8 sequences for mutant and plasmid generation are given in Supplementary Table 3. Strains of *S.*
9 *marcescens* were grown at 30°C in LB media (10 g/l tryptone, 5 g/l yeast extract, 10 g/l NaCl),
10 solidified with 12 g/l agar or supplemented with antibiotics (kanamycin, 100 µg/ml; streptomycin, 100
11 µg/ml) where required.

12 **Fungal strains, plasmids and culture conditions**

13 Fungal strains and plasmids are given in Supplementary Table 2. To generate mutant strains of *S.*
14 *cerevisiae* K699 carrying chromosomal insertions of GFP or bacterial effector genes under the control
15 of the P_{GALI} promoter, linearized plasmids pSC1384 (control), pSC1379 (GFP), pSC1382 (Tfe1) and
16 pSC1380 (Tfe2), all based on plasmid pGED1, were integrated by allelic exchange into the HIS3
17 locus. Plasmid-based gene expression utilised the galactose-inducible vector pRB1438. For *in trans*
18 expression of bacterial effectors in *C. albicans*, chromosomal integration mutants based on the
19 doxycycline-inducible expression vector pNIM1¹⁸ were generated. To ensure correct leucine
20 incorporation into the expressed protein in *C. albicans*, synthetic genes carrying CTG to TTG
21 substitutions (Invitrogen) were subcloned into pNIM1. Correct sequence and locus integration was
22 confirmed by sequencing of the respective PCR product, together with Southern blot analysis for *C.*
23 *albicans*. All primer sequences for mutant and plasmid generation and Southern blot probe generation
24 are given in Supplementary Table 3. Fungal strains were cultured at 30°C in YPA (10g/l yeast extract,
25 20g/l peptone, 40 mg/l adenine hemisulfate) or synthetic complete (SC; 6.9 g/l yeast nitrogen base
26 complete with ammonium sulfate and amino acids) media containing 2% glucose⁴⁹. If utilizing
27 auxotrophies, SC media lacking the respective amino acid or nucleotide was used. For induction of
28 the P_{GALI} promoter, *S. cerevisiae* cultures were pre-incubated in media containing 2% raffinose,

1 washed, and incubated with media containing both 2% galactose and 2% raffinose unless otherwise
2 stated. Induction of the Tet-inducible promoter in *C. albicans* was by addition of 50 µg/ml
3 doxycycline.

4 **Co-culture assay for T6SS-mediated anti-fungal activity**

5 Anti-fungal activity assays were based on the anti-bacterial co-culture assay described previously¹⁰.
6 Both the attacker strain derived from *S. marcescens* Db10 and the respective fungal target strain were
7 normalized to an OD₆₀₀ of 1, mixed at a volume ratio of 1:1 (attacker:target cell ratio ~100:1), and
8 12.5 µl of the mixture were spotted on solid SC + 2% glucose media and incubated for 7.5 h at 30°C.
9 Surviving target fungal cells were enumerated by serial dilution and viable counts on streptomycin-
10 supplemented YPDA media. Co-culture assays for anti-bacterial activity were performed as
11 described^{10, 16}. For assessment of cell contact dependence, bacterial and fungal cells were separated by
12 a membrane (pore size 0.22 µm), with the bacterial layer between the solid medium and the
13 membrane and the fungal cells spotted on top of the membrane. *S. cerevisiae* grew equally well on the
14 membrane placed on top of the bacterial cell layer compared with direct growth on the medium,
15 confirming efficient diffusion of nutrients through the membrane. The co-culture experiments
16 presented contain data from four independent biological replicates, performed on at least two days,
17 with T6SS-dependent anti-fungal activity and the phenotypes of the $\Delta tfe1$ and $\Delta tfe2$ mutants having
18 been confirmed on multiple independent occasions.

19 **Plate toxicity assay**

20 Fungal cells were pre-grown in non-inducing liquid minimal media (SC + 2% glucose, *C. albicans*;
21 DOA-LEU + 2% raffinose, *S. cerevisiae*) at 30°C, adjusted to an OD₆₀₀ of 1, serially diluted and 5 µl
22 spotted onto minimal media agar. Heterologous protein expression was induced by addition of
23 doxycycline (50 µg/ml, *C. albicans*) or galactose (0.008 – 0.2%, *S. cerevisiae*). Agar plates were
24 incubated at 30°C and pictures taken after 48 h (*C. albicans*) or 96 h (*S. cerevisiae*).

25 **Cell morphology and viability analysis by microscopy**

26 Single cell morphology of fungal cells grown in co-culture (7.5 h) or in liquid induction media (SC +
27 2% glucose + 50 µg/ml doxycycline, *C. albicans*; DOA-URA + 2% raffinose + 2% galactose, *S.*
28 *cerevisiae*; 8h) was visualized by differential interference contrast (DIC) using a Axio-Imager M1

1 microscope equipped with a 100x objective, AxioCam MRm camera and ZEN software (Zeiss). The
2 images presented show multiple individual cells from part of one field of view, for clarity, and are
3 representative of between 9 and 42 fields of view, acquired on three separate occasions. To determine
4 the percentage of PI-stained fungal cells, cells from three independent fungal-bacterial co-cultures
5 grown at 30°C for 7.5 h on solid SC + 2% glucose media were recovered in 1x PBS and stained with
6 PI at a final concentration of 10 µg/ml. Following a 15 min incubation at 30°C, 1.5 µl of the stained
7 cell suspension were placed on a microscope slide layered with a 1% agarose pad and cells were
8 detected by both DIC and fluorescence microscopy using a HBO 100 mercury lamp and appropriate
9 filter sets (Ex 546/12 nm, Em 607/65 nm) and 40x objective. A minimum of 160 cells per
10 experimental condition and replicate were scored, with the aid of the counting tool in
11 OMERO.mtools⁵⁰. Cells subjected to a 40 min heat-shock at 65°C served as positive control for PI
12 staining. Visualisation of *C. albicans* hyphae was performed using a Zeiss Axioskop 2 MOT
13 microscope, 63x objective, HBO100 mercury lamp and Zeiss AxioCam Color camera, following
14 incubation with 1 µM propidium iodide for 10 min. Microscopy images were managed and processed
15 according to accepted standards using OMERO (<http://openmicroscopy.org>)⁵⁰ and Fiji⁵¹.

16 **Microscopy analysis of metabolic activity and membrane potential**

17 For staining of effector-expressing *S. cerevisiae* cells using FUN1, cells were grown in synthetic drop-
18 out media (DOA-LEU) supplemented with 2% raffinose, washed once, normalized to an OD₆₀₀ of 0.5
19 and expression induced by addition of 2% galactose for 9 h. Cells were washed, suspended in 10 mM
20 HEPES, pH 7.2, 2% raffinose, 2% galactose, stained with FUN1 (Thermo Fisher, dilution 1:1;000) for
21 30 min at 30°C, and analysed by DIC and fluorescence microscopy using appropriate filter sets (green,
22 Ex 470/40 nm, Em 525/50 nm, 40 ms exposure; and red, Ex 546/12 nm, Em 607/65 nm, 150 ms
23 exposure) on the Axio-Imager described above. Multiple fields of view were imaged and the experiment
24 has been reproduced on an independent occasion.

25 To visualise and distinguish between changes in plasma membrane potential and membrane diffusion
26 barrier function, *S. cerevisiae* cells grown in liquid induction media (DOA-URA + 2% raffinose + 2%
27 galactose; 6 h) were placed on a microscope slide layered with a 1% agarose pad containing the voltage-
28 dependent dye Bis-(1,3-dibutylbarbituric acid) trimethine oxonol [DiBAC₄(3)] (AnaSpec) at a final

1 concentration of 10 μ M, either alone, or combined with the membrane permeability-reporter propidium
2 iodide (Sigma) added at a final concentration of 1 μ M. To suppress binding of DiBAC₄(3) on the glass
3 surface, the coverslips were coated with L-dopamine⁵². Amphotericin B (Sigma), used as positive
4 control to induce membrane depolarization without pore formation, was added to control cells at the
5 start of the 6 h induction period at a final concentration of 3 μ g/ml. The pore-forming peptide mellitin
6 (AnaSpec) was added to the cells 10 min prior to the end of the 6 h induction period at a final
7 concentration of 100 μ M. Fluorescence and phase contrast microscopy was carried out with Nikon
8 Eclipse Ti equipped with Nikon Plan Apo 100x/1.40 Oil Ph3 objective, Sutter Instrument Company
9 Lambda LS xenon arc light source, and Photometrics Prime sCMOS camera using appropriate filter
10 sets (green Ex 470/40 nm, Em 525/50 nm, 500 ms exposure; and red Ex 560/40 nm, 630/40 nm, 100
11 ms exposure). The images were captured using Metamorph 7.7 (Molecular Devices). Multiple fields of
12 view were imaged and the experiment has been reproduced on an independent occasion. The
13 quantification of cell fluorescence levels was performed by automated detection of cells using phase
14 contrast images, followed by measurement of whole cell DiBAC₄(3) and Propidium iodide average
15 fluorescence intensities from corresponding, background-subtracted fluorescent micrographs. The cell
16 detection and fluorescence intensity measurements were carried out using Fiji⁵¹.

17 **Immunoblot analysis**

18 Anti-Hcp and anti-Ssp2 immunoblots were performed on cultures grown for 5 h as previously
19 described^{10, 16}. Polyclonal anti-Hcp¹⁰ and anti-Ssp2¹⁶ primary antibodies were used at 1:6,000 and
20 1:2,000 respectively, with peroxidase-conjugated anti-rabbit secondary antibody (BioRad) at
21 1:10,000. Cellular samples for immunodetection of GFP-Atg8 and Pgk1 were prepared from yeast-
22 bacterial co-cultures based on⁵³. Yeast cells were harvested from co-cultures grown at 30°C for 7.5 h
23 on solid SC + 2% glucose media into ice-cold phosphate buffered saline (PBS; 8 g/l NaCl, 0.2 g/l
24 KCl, 1.42 g/l Na₂HPO₄, 0.24 g/l KH₂PO₄, pH 7.4), washed twice by filtering through 3 μ m pore-sized
25 PVDF membranes (Millipore) and recovered by centrifugation. For subsequent protein extraction, cell
26 pellets were resuspended and incubated for 10 min in 0.2 M NaOH, 1% β -mercaptoethanol. Proteins
27 were precipitated by addition of trichloroacetic acid (TCA; 20% final concentration), washed once in
28 ice-cold acetone, resuspended in 2x SDS sample buffer (100 mM Tris-HCl, pH 6.8, 3.2% SDS, 3.2

1 mM EDTA, 16% glycerol, 0.2 mg/ml bromophenol blue and 2.5% β -mercaptoethanol) and boiled for
2 10 min before being subjected to western blot analysis. Due to the growth impediment of *S. cerevisiae*
3 in the presence of *S. marcescens* Db10 and residual bacterial contamination of yeast samples, protein
4 extracts were normalized according to the abundance of the protein Pgk1. Monoclonal anti-GFP (cat #
5 11814460001, Roche) and polyclonal anti-Pgk1 (cat # 13472727, Invitrogen) primary antibodies were
6 used at 1:5,000 and 1:1,000 respectively, with peroxidase-conjugated anti-mouse and anti-rabbit
7 secondary antibodies (BioRad) at 1:10,000.

8 **Quantitative real-time PCR**

9 RNA was extracted from three independent cultures of control and Tfe2-expressing *S. cerevisiae*
10 cells, induced for 6 h at 30°C in galactose induction media, using the SV Total RNA Isolation System
11 (Promega), followed by treatment with the Turbo DNA-free kit (Ambion) to remove residual gDNA.
12 RNA was reverse transcribed using the iScript cDNA Synthesis Kit (Bio-Rad) and relative levels of
13 cDNA determined using an Mx3005P QPCR machine (Stratagene, Agilent Technologies) with actin
14 (*ACT1*) as the normalizing gene. Primer sequences are given in Supplementary Table 3. The
15 experiment presented has been reproduced on an independent occasion.

16 **Whole-cell amino acid analysis**

17 Three independent cultures of control and Tfe2-expressing *S. cerevisiae* cells were incubated for 6 h
18 at 30°C in galactose induction media, washed twice with ice-cold water, normalized to 5 OD₆₀₀ per 1
19 ml of water and boiled for 15 min. After centrifugation, the supernatant was clarified using a 0.2 μ m
20 syringe filter (Sartorius). The resulting extract was acidified by addition of TFA in MeOH (10%, v/v),
21 dried and resuspended in buffer (40% 1M NaOAc, 40% MeOH, 20% triethylamine, TEA), before
22 being dried again. The amino acids were then derivatized using Phenylisothiocyanate (PITC) by
23 resuspension of the dried material in 10% PITC, 70% MeOH, 10% H₂O, 10% TEA, followed by 2-
24 fold dilution in MeOH. After 15 min incubation at room temperature, suspensions were dried, washed
25 once with MeOH and suspended in elution buffer, composed of 95% (150 mM NaOAc, 0.5 ml/l TEA,
26 pH 6.4) and 5% acetonitrile. PTC amino acid derivatives were analysed by HPLC using a Nova-Pak®
27 C18 column (Waters), the Clarity Lite software and two amino acid standard sets (AA-S-18 and
28 A6282, Sigma). The experiment presented has been reproduced on two independent occasions.

1 **Sample preparation for mass spectrometry**

2 For analysis of the cellular proteome of *S. marcescens*, six biological replicates of each strain (two
3 spots of 25 μ l of OD₆₀₀ 0.5 per replicate) were grown on solid LB media for 7.5 h at 30°C. Cells were
4 recovered, washed in ice-cold PBS, resuspended in 1% sodium 3-[(2-methyl-2-undecyl-1,3-dioxolan-
5 4-yl)methoxy]-1-propanesulfonate (commercially available as RapiGest, Waters, Milford, MA), 50
6 mM Tris-HCl pH 8.0, 1 mM tris(2-carboxyethyl)phosphine (TCEP) and lysed by sonication.

7 For analysis of bacterially-intoxicated fungal cells, co-cultures of *C. albicans* and *S. marcescens* (57
8 co-culture spots, inoculated as above, per replicate) were incubated on solid SC + 2% glucose media
9 for 4 h at 30°C, with six biological replicates per combination. Cells were harvested in 40 ml ice-cold
10 PBS, washed 2x by filtration using PVDF membranes, pore size 3 μ m (Millipore), suspended in PBS
11 and recovered by centrifugation. Cells were sonicated in 1% Rapigest, 50 mM Tris-HCl pH 8.0, 1
12 mM TCEP in the presence of 0.1 mm zirconia/silica beads (BioSpec) for 6x 10 sec with 20 sec
13 intervals. In each study, following sonication, samples were heated for 5 min at 95°C and soluble
14 protein extracts recovered by centrifugation.

15 Protein concentrations were determined using the EZQ Kit (Thermo-Fisher Scientific) and cysteines
16 were alkylated by addition of 5 mM iodoacetamide. After 20 min incubation in the dark at 25°C, the
17 reaction was quenched by addition of 5 mM DTT and samples were diluted 10x in 50 mM Tris-HCl
18 pH 8.0. Digestion of proteins was by addition of trypsin (MS grade, Pierce, Thermo-Fisher) at a 1:150
19 (w/w) ratio with incubation overnight at 37°C, followed by a second addition of trypsin (1:150 w/w)
20 with 3 h incubation. Rapigest was cleaved by addition of 2% trifluoroacetic acid (TFA) and
21 incubation for 1 h at 37°C. Samples were desalted using C18 columns (Harvard Apparatus) and
22 lyophilised.

23 **Mass spectrometry analysis of *Serratia marcescens* cellular proteome**

24 Lyophilised peptide samples (six biological replicates) were taken up in 2% acetonitrile (ACN), 0.1%
25 TFA and analysed similar to previously published methods⁵⁴⁻⁵⁶: separated on an Ultimate 3000 RSLC
26 system (Thermo-Fisher Scientific) with a C18 PepMap, serving as a trapping column (2 cm x 100 μ m
27 ID, PepMap C18, 5 μ m particles, 100 Å pore size) followed by a 50 cm EASY-Spray column (50 cm
28 x 75 μ m ID, PepMap C18, 2 μ m particles, 100 Å pore size; Thermo-Fisher Scientific) with a 6 h

1 gradient consisting of 3-30% B (B= 80% ACN, 0.1% formic acid (FA); 10-260 min), to 40% B (330
2 min), 99% B (335-345 min), 3% (350-360 min) at 300 nl/min. Mass spectrometric identification and
3 quantification was performed on an Orbitrap Velos mass spectrometer (Thermo-Fisher Scientific)
4 operated in data dependent, positive ion mode. FullScan spectra were acquired in a range from 350
5 m/z to 1600 m/z, at a resolution of 60,000. MS/MS in the ion trap was triggered for ions above 2000
6 with a maximum injection time of 10 ms for the 20 most intense precursor ions in RapidScan and a
7 lockmass of 445.120024. Collision-induced dissociation (CID) fragmentation was performed at a
8 collision energy of 35% and 0.25 activation Q.

9 Label-free protein identification and quantification were performed using MaxQuant version 1.4.1.2⁵⁷
10 with the following parameters: stable modification carbamidomethyl (C); variable modifications
11 oxidation (M), acetylation (protein N terminus), and trypsin as enzyme with 2 missed cleavages.
12 Search was conducted using a combined FASTA database of *Serratia marcescens* Db11 and the
13 Uniprot *Homo sapiens* database (downloaded May 1st 2013), including common contaminants. Mass
14 accuracy was set to 4.5 ppm for precursor ions and 0.5 Da for ion trap MS/MS data. Identifications
15 were filtered at a 1% false-discovery rate (FDR) at the protein and peptide level, accepting a
16 minimum peptide length of 7 amino acids. Quantification of identified proteins referred to razor and
17 unique peptides, and required a minimum ratio count of 2. Normalized ratios were extracted for each
18 protein and were used for downstream analyses.

19 **'In competition' proteomics of bacterially-intoxicated *C. albicans***

20 Isobaric labelling of peptides was performed using 6-plex tandem mass tag (TMT) reagents (Thermo-
21 Fisher Scientific). TMT reagents (0.8 mg) were dissolved in 40 µl of acetonitrile and 20 µl was added
22 to six biological replicates of lyophilised peptide samples, previously dissolved in 50 µl of 50 mM
23 triethylammonium bicarbonate, pH 8.0. The individual samples of the strains were labelled as follows
24 for all six replicates: WT, 126; $\Delta tssE$, 127; $\Delta tfe1$, 128; $\Delta tfe2$, 129; $\Delta tfe1\Delta tfe2$, 130. After labelling,
25 the reaction was quenched by addition of 4 µl of 5% hydroxylamine after 1 hour incubation at room
26 temperature. Individual samples were tested for labelling efficiency (>95%) before the labelled
27 peptides were combined, acidified with 0.1% TFA and concentrated using C18 SPE on Sep-Pak
28 cartridges (Waters). Equal loading of all five conditions was confirmed by the majority of peptide

1 intensities not changing before normalisation.

2 TMT labelled peptides were subjected to hydrophilic Strong Anion Exchange (hSAX) fractionation.⁵⁸

3 Labelled peptides were solubilized in 20 mM Tris-HCl, pH 10.0) and separated on a Dionex RFIC

4 IonPac AS24 column (IonPac series, 2 × 250 mm, 2000 Å pore size; Thermo-Fisher Scientific). Using

5 a DGP-3600BM pump system equipped with a SRD-3600 degasser (Thermo-Fisher Scientific) a 30

6 min gradient length from 8% to 80% of 1M NaCl in 20 mM Tris-HCl, pH 10 (flow rate of 0.25

7 ml/min), separated the peptide mixtures into a total of 34 fractions. The 34 fractions were merged into

8 9 samples, acidified with 1 %TFA (pH = 2), desalted via C18 Macro SpinColumns (Harvard

9 Apparatus), dried under vacuum centrifugation and re-suspended in 2% ACN / 0.1% TFA for LC-

10 MS/MS analysis.

11 Peptide samples were separated on an Ultimate 3000 RSLC system with a C18 PepMap, serving as a

12 trapping column (2 cm x 100 µm ID, PepMap C18, 5 µm particles, 100 Å pore size) followed by a 50

13 cm EASY-Spray column with a linear gradient consisting of (2.4-28% ACN, 0.1% FA) over 150 min

14 at 300 nl/min. Mass spectrometric identification and quantification was performed on an Orbitrap

15 Fusion Tribrid mass spectrometer (Thermo-Fisher Scientific) operated in data dependent, positive ion

16 mode. FullScan spectra were acquired in a range from 400 m/z to 1500 m/z, at a resolution of

17 120,000, with an automated gain control (AGC) of 300,000 ions and a maximum injection time of 50

18 ms. The 12 most intense precursor ions were isolated with a quadrupole mass filter width of 1.6 m/z

19 and CID fragmentation was performed in one-step collision energy of 32% and 0.25 activation Q.

20 Detection of MS/MS fragments was acquired in the linear ion trap in a rapid mode with an AGC

21 target of 10,000 ions and a maximum injection time of 40 ms. Quantitative analysis of TMT-tagged

22 peptides was performed using FTMS3 acquisition in the Orbitrap mass analyser operated at 60,000

23 resolution, with an AGC target of 100,000 ions and maximum injection time of 120 ms. Higher-

24 energy C-trap dissociation (HCD fragmentation) on MS/MS fragments was performed in one-step

25 collision energy of 55% to ensure maximal TMT reporter ion yield and synchronous-precursor-

26 selection (SPS) was enabled to include 10 MS/MS fragment ions in the FTMS3 scan.

27 Protein identification and quantification were performed using MaxQuant version 1.5.1.7⁵⁷ with the

28 following parameters: stable modification carbamidomethyl (C); variable modifications oxidation

1 (M), acetylation (protein N terminus), deamidation (NQ), hydroxyproline (P), quantitation labels with
2 6plex TMT on N-terminal or lysine with a reporter mass tolerance of 0.01 Da and trypsin as enzyme
3 with 2 missed cleavages. Search was conducted using a combined FASTA database of *Serratia*
4 *marcescens* Db11 and the *Candida albicans* SC5314 (assembly 22) database⁵⁹ (downloaded from
5 www.candidagenome.org on September 1st 2015), including common contaminants. Mass accuracy
6 was set to 4.5 ppm for precursor ions and 0.5 Da for ion trap MS/MS data. Identifications were
7 filtered at a 1% FDR at the protein and peptide level, accepting a minimum peptide length of 7 amino
8 acids. Quantification of identified proteins referred to razor and unique peptides, and required a
9 minimum ratio count of 2. Normalized ratios were extracted for each protein/conditions and were
10 used for downstream analyses.

11 **Mass spectrometry data analysis**

12 Data was further analysed using the Perseus software package⁶⁰. Pairwise comparisons were made
13 using Student's T-tests ($p < 0.05$, two-tailed). Multiple samples were analysed using ANOVA at
14 $p < 0.05$. Perseus was also used for heatmaps and clustering (Euclidean, 10 clusters) of ANOVA
15 positive proteins. For the *S. marcescens* cellular proteome, proteins were identified as differentially
16 abundant when at least two unique peptides were identified, intensities were detected in a minimum of
17 two out of the six biological replicates, and average LFQ intensities were altered more than 1.4-fold
18 ($|\log_2| > 0.5$, $p\text{-value} < 0.05$). For the bacterially-intoxicated *C. albicans* proteome, modulated
19 proteins had significant ANOVA score (two-sided, $p\text{-value} < 0.05$) and strong effector-specific
20 changes were identified by pairwise comparison (fold change > 1.3 , $p\text{-value} < 0.05$). Gene Ontology
21 (GO) term analysis was carried out using the GO Term Finder Tool applying standard settings
22 available at Candida Genome Database (CGD)⁶¹ (<http://www.candidagenome.org/>).

23 **Data availability**

24 Raw mass spectrometry data that support the findings of this study have been deposited to the
25 ProteomeXchange Consortium via the PRIDE⁶² partner repository with the dataset identifier
26 PXD006916. All other data supporting the findings of this study are available within the paper and its
27 supplementary information files.

1 References

- 2 1. Boer, W., Folman, L.B., Summerbell, R.C. & Boddy, L. Living in a fungal world: impact of
3 fungi on soil bacterial niche development. *FEMS Microbiol Rev* **29**, 795-811 (2005).
- 4 2. Peleg, A.Y., Hogan, D.A. & Mylonakis, E. Medically important bacterial-fungal interactions.
5 *Nat Rev Microbiol* **8**, 340-349 (2010).
- 6 3. Costa, T.R. *et al.* Secretion systems in Gram-negative bacteria: structural and mechanistic
7 insights. *Nat Rev Microbiol* **13**, 343-359 (2015).
- 8 4. Basler, M. Type VI secretion system: secretion by a contractile nanomachine. *Philos Trans R*
9 *Soc Lond B Biol Sci* **370** (2015).
- 10 5. Cianfanelli, F.R., Monlezun, L. & Coulthurst, S.J. Aim, Load, Fire: The Type VI Secretion
11 System, a Bacterial Nanoweapon. *Trends Microbiol* **24**, 51-62 (2016).
- 12 6. Durand, E., Cambillau, C., Cascales, E. & Journet, L. VgrG, Tae, Tle, and beyond: the
13 versatile arsenal of Type VI secretion effectors. *Trends Microbiol* **22**, 498-507 (2014).
- 14 7. Hachani, A., Wood, T.E. & Filloux, A. Type VI secretion and anti-host effectors. *Curr Opin*
15 *Microbiol* **29**, 81-93 (2016).
- 16 8. Alcoforado Diniz, J., Liu, Y.C. & Coulthurst, S.J. Molecular weaponry: diverse effectors
17 delivered by the Type VI secretion system. *Cell Microbiol* **17**, 1742-1751 (2015).
- 18 9. Russell, A.B., Peterson, S.B. & Mougous, J.D. Type VI secretion system effectors: poisons
19 with a purpose. *Nat Rev Microbiol* **12**, 137-148 (2014).
- 20 10. Murdoch, S.L. *et al.* The opportunistic pathogen *Serratia marcescens* utilizes type VI
21 secretion to target bacterial competitors. *J Bacteriol* **193**, 6057-6069 (2011).
- 22 11. Klis, F.M., de Koster, C.G. & Brul, S. Cell wall-related biomarkers and bioestimates of
23 *Saccharomyces cerevisiae* and *Candida albicans*. *Eukaryot Cell* **13**, 2-9 (2014).
- 24 12. Fritsch, M.J. *et al.* Proteomic identification of novel secreted antibacterial toxins of the
25 *Serratia marcescens* type VI secretion system. *Mol Cell Proteomics* **12**, 2735-2749 (2013).
- 26 13. Peters, B.M., Jabra-Rizk, M.A., O'May, G.A., Costerton, J.W. & Shirliff, M.E. Polymicrobial
27 interactions: impact on pathogenesis and human disease. *Clin Microbiol Rev* **25**, 193-213
28 (2012).
- 29 14. Turner, S.A. & Butler, G. The *Candida* pathogenic species complex. *Cold Spring Harb*
30 *Perspect Med* **4**, a019778 (2014).
- 31 15. Cianfanelli, F.R. *et al.* VgrG and PAAR Proteins Define Distinct Versions of a Functional
32 Type VI Secretion System. *PLoS Pathog* **12**, e1005735 (2016).
- 33 16. English, G. *et al.* New secreted toxins and immunity proteins encoded within the Type VI
34 secretion system gene cluster of *Serratia marcescens*. *Mol Microbiol* **86**, 921-936 (2012).
- 35 17. Murdoch, S.L. *et al.* The opportunistic pathogen *serratia marcescens* utilizes type VI secretion
36 to target bacterial competitors. *J Bacteriol* **193**, 6057-6069 (2011).
- 37 18. Park, Y.N. & Morschhauser, J. Tetracycline-inducible gene expression and gene deletion in
38 *Candida albicans*. *Eukaryot Cell* **4**, 1328-1342 (2005).
- 39 19. Millard, P.J., Roth, B.L., Thi, H.P., Yue, S.T. & Haugland, R.P. Development of the FUN-1
40 family of fluorescent probes for vacuole labeling and viability testing of yeasts. *Appl Environ*
41 *Microbiol* **63**, 2897-2905 (1997).
- 42 20. Essary, B.D. & Marshall, P.A. Assessment of FUN-1 vital dye staining: Yeast with a block in
43 the vacuolar sorting pathway have impaired ability to form CIVS when stained with FUN-1
44 fluorescent dye. *J Microbiol Methods* **78**, 208-212 (2009).
- 45 21. Hogan, D.A. & Kolter, R. *Pseudomonas-Candida* interactions: an ecological role for virulence
46 factors. *Science* **296**, 2229-2232 (2002).
- 47 22. Braun, B.R. & Johnson, A.D. Control of filament formation in *Candida albicans* by the
48 transcriptional repressor TUP1. *Science* **277**, 105-109 (1997).
- 49 23. Marzluf, G.A. Molecular genetics of sulfur assimilation in filamentous fungi and yeast. *Annu*
50 *Rev Microbiol* **51**, 73-96 (1997).
- 51 24. Kraidlova, L. *et al.* Characterization of the *Candida albicans* Amino Acid Permease Family:
52 Gap2 Is the Only General Amino Acid Permease and Gap4 Is an S-Adenosylmethionine
53 (SAM) Transporter Required for SAM-Induced Morphogenesis. *mSphere* **1** (2016).

- 1 25. Sychrova, H. & Souciet, J.L. CAN1, a gene encoding a permease for basic amino acids in
2 Candida albicans. *Yeast* **10**, 1647-1651 (1994).
- 3 26. Matijekova, A. & Sychrova, H. Biogenesis of Candida albicans Can1 permease expressed in
4 Saccharomyces cerevisiae. *FEBS Lett* **408**, 89-93 (1997).
- 5 27. Ljungdahl, P.O. & Daignan-Fornier, B. Regulation of amino acid, nucleotide, and phosphate
6 metabolism in Saccharomyces cerevisiae. *Genetics* **190**, 885-929 (2012).
- 7 28. Ljungdahl, P.O. Amino-acid-induced signalling via the SPS-sensing pathway in yeast.
8 *Biochem Soc Trans* **37**, 242-247 (2009).
- 9 29. Brega, E., Zufferey, R. & Mamoun, C.B. Candida albicans Csy1p is a nutrient sensor
10 important for activation of amino acid uptake and hyphal morphogenesis. *Eukaryot Cell* **3**,
11 135-143 (2004).
- 12 30. Didion, T., Regenber, B., Jorgensen, M.U., Kielland-Brandt, M.C. & Andersen, H.A. The
13 permease homologue Ssy1p controls the expression of amino acid and peptide transporter
14 genes in Saccharomyces cerevisiae. *Mol Microbiol* **27**, 643-650 (1998).
- 15 31. Iraqui, I. *et al.* Amino acid signaling in Saccharomyces cerevisiae: a permease-like sensor of
16 external amino acids and F-Box protein Grr1p are required for transcriptional induction of the
17 AGP1 gene, which encodes a broad-specificity amino acid permease. *Mol Cell Biol* **19**, 989-
18 1001 (1999).
- 19 32. Klasson, H., Fink, G.R. & Ljungdahl, P.O. Ssy1p and Ptr3p are plasma membrane
20 components of a yeast system that senses extracellular amino acids. *Mol Cell Biol* **19**, 5405-
21 5416 (1999).
- 22 33. Tripathi, G. *et al.* Gcn4 co-ordinates morphogenetic and metabolic responses to amino acid
23 starvation in Candida albicans. *EMBO J* **21**, 5448-5456 (2002).
- 24 34. Hinnebusch, A.G. Mechanisms of gene regulation in the general control of amino acid
25 biosynthesis in Saccharomyces cerevisiae. *Microbiol Rev* **52**, 248-273 (1988).
- 26 35. Reggiori, F. & Klionsky, D.J. Autophagic processes in yeast: mechanism, machinery and
27 regulation. *Genetics* **194**, 341-361 (2013).
- 28 36. Guan, J. *et al.* Cvt18/Gsa12 is required for cytoplasm-to-vacuole transport, pexophagy, and
29 autophagy in Saccharomyces cerevisiae and Pichia pastoris. *Mol Biol Cell* **12**, 3821-3838
30 (2001).
- 31 37. Delorme-Axford, E., Guimaraes, R.S., Reggiori, F. & Klionsky, D.J. The yeast
32 Saccharomyces cerevisiae: an overview of methods to study autophagy progression. *Methods*
33 **75**, 3-12 (2015).
- 34 38. Cebollero, E. & Reggiori, F. Regulation of autophagy in yeast Saccharomyces cerevisiae.
35 *Biochim Biophys Acta* **1793**, 1413-1421 (2009).
- 36 39. Rubin-Bejerano, I., Fraser, I., Grisafi, P. & Fink, G.R. Phagocytosis by neutrophils induces an
37 amino acid deprivation response in Saccharomyces cerevisiae and Candida albicans. *Proc*
38 *Natl Acad Sci U S A* **100**, 11007-11012 (2003).
- 39 40. Fradin, C. *et al.* Granulocytes govern the transcriptional response, morphology and
40 proliferation of Candida albicans in human blood. *Mol Microbiol* **56**, 397-415 (2005).
- 41 41. Lorenz, M.C., Bender, J.A. & Fink, G.R. Transcriptional response of Candida albicans upon
42 internalization by macrophages. *Eukaryot Cell* **3**, 1076-1087 (2004).
- 43 42. Jimenez-Lopez, C. *et al.* Candida albicans induces arginine biosynthetic genes in response to
44 host-derived reactive oxygen species. *Eukaryot Cell* **12**, 91-100 (2013).
- 45 43. Basler, M., Pilhofer, M., Henderson, G.P., Jensen, G.J. & Mekalanos, J.J. Type VI secretion
46 requires a dynamic contractile phage tail-like structure. *Nature* **483**, 182-186 (2012).
- 47 44. Dupres, V., Dufrene, Y.F. & Heinisch, J.J. Measuring cell wall thickness in living yeast cells
48 using single molecular rulers. *ACS Nano* **4**, 5498-5504 (2010).
- 49 45. Yamaguchi, M. *et al.* Structome of Saccharomyces cerevisiae determined by freeze-
50 substitution and serial ultrathin-sectioning electron microscopy. *J Electron Microsc (Tokyo)*
51 **60**, 321-335 (2011).
- 52 46. Hoarau, G. *et al.* Bacteriome and Mycobiome Interactions Underscore Microbial Dysbiosis in
53 Familial Crohn's Disease. *MBio* **7** (2016).
- 54 47. Mahlen, S.D. Serratia infections: from military experiments to current practice. *Clin*
55 *Microbiol Rev* **24**, 755-791 (2011).

- 1 48. Haapalainen, M. *et al.* Hcp2, a secreted protein of the phytopathogen *Pseudomonas syringae*
2 pv. tomato DC3000, is required for fitness for competition against bacteria and yeasts. *J*
3 *Bacteriol* **194**, 4810-4822 (2012).
4
5

6 **References for Methods Section**

7

- 8 49. Amberg, D.C., Burke, D., Strathern, J.N., Burke, D. & Cold Spring Harbor Laboratory.
9 *Methods in yeast genetics : a Cold Spring Harbor Laboratory course manual*, Edn. 2005.
10 (Cold Spring Harbor Laboratory Press, New York; 2005).
11 50. Allan, C. *et al.* OMERO: flexible, model-driven data management for experimental biology.
12 *Nat Methods* **9**, 245-253 (2012).
13 51. Schindelin, J. *et al.* Fiji: an open-source platform for biological-image analysis. *Nat Methods*
14 **9**, 676-682 (2012).
15 52. te Winkel, J.D., Gray, D.A., Seistrup, K.H., Hamoen, L.W. & Strahl, H. Analysis of
16 Antimicrobial-Triggered Membrane Depolarization Using Voltage Sensitive Dyes. *Frontiers*
17 *in Cell and Developmental Biology* **4** (2016).
18 53. Knop, M. *et al.* Epitope tagging of yeast genes using a PCR-based strategy: more tags and
19 improved practical routines. *Yeast* **15**, 963-972 (1999).
20 54. Naujoks, J. *et al.* IFNs Modify the Proteome of Legionella-Containing Vacuoles and Restrict
21 Infection Via IRG1-Derived Itaconic Acid. *PLoS Pathog.* **12**, e1005408 (2016).
22 55. Guo, M. *et al.* High-resolution quantitative proteome analysis reveals substantial differences
23 between phagosomes of RAW 264.7 and bone marrow derived macrophages. *Proteomics* **15**,
24 3169-3174 (2015).
25 56. Dill, B.D. *et al.* Quantitative proteome analysis of temporally resolved phagosomes following
26 uptake via key phagocytic receptors. *Mol. Cell. Proteomics* **14**, 1334-1349 (2015).
27 57. Cox, J. & Mann, M. MaxQuant enables high peptide identification rates, individualized
28 p.p.b.-range mass accuracies and proteome-wide protein quantification. *Nat. Biotechnol.* **26**,
29 1367-1372 (2008).
30 58. Ritorto, M.S., Cook, K., Tyagi, K., Pedrioli, P.G. & Trost, M. Hydrophilic strong anion
31 exchange (hSAX) chromatography for highly orthogonal peptide separation of complex
32 proteomes. *J. Proteome Res.* **12**, 2449-2457 (2013).
33 59. Muzzey, D., Schwartz, K., Weissman, J.S. & Sherlock, G. Assembly of a phased diploid
34 *Candida albicans* genome facilitates allele-specific measurements and provides a simple
35 model for repeat and indel structure. *Genome Biol.* **14**, R97 (2013).
36 60. Tyanova, S. *et al.* The Perseus computational platform for comprehensive analysis of
37 (prote)omics data. *Nat. Methods* **13**, 731-740 (2016).
38 61. Skrzypek, M.S. *et al.* The *Candida* Genome Database (CGD): incorporation of Assembly 22,
39 systematic identifiers and visualization of high throughput sequencing data. *Nucleic Acids Res*
40 **45**, D592-D596 (2017).
41 62. Vizcaino, J.A. *et al.* 2016 update of the PRIDE database and its related tools. *Nucleic Acids*
42 *Res* **44**, D447-456 (2016).

43

1 **Correspondence and requests for material** should be addressed to S.J.C. or M.T.

2

3 **Acknowledgements**

4 This work was supported by the Wellcome Trust (Senior Research Fellowship in Basic Biomedical
5 Science to S.J.C., 104556; 097377, J.Q.; 101873 & 200208, N.A.R.G.), the MRC (MR/K000111X/1,
6 S.J.C; MC_UU_12016/5, M.T.), and the BBSRC (BB/K016393/1 & BB/P020119/1, J.Q.). We thank
7 Maximilian Fritsch, Mario López Martín and Birte Hollmann for help with strain construction; Gary
8 Eitzen for construction of pGED1; Donna MacCallum for the gift of *Candida glabrata* ATCC2001;
9 Joachim Morschhäuser for the gift of pNIM1; Gillian Milne (Microscopy and Histology facility,
10 University of Aberdeen) for assistance with TEM; and Peter Taylor, Michael Porter, Laura Monlezun
11 and Colin Rickman for advice and technical assistance.

12

13 **Author Contributions**

14 K.T., M.T. and S.J.C conceived the study and designed experiments; K.T., J.P., Y.L., B.D.D., L.W.
15 and H.S. performed experimental work, J.P. and H.S. additionally performed data analysis; J.Q.,
16 M.J.R.S and N.A.R.G. contributed expertise and reagents; K.T., M.T and S.J.C. analysed data and
17 wrote the manuscript.

18

19 **Competing Financial Interests**

20 The authors declare no competing financial interests.

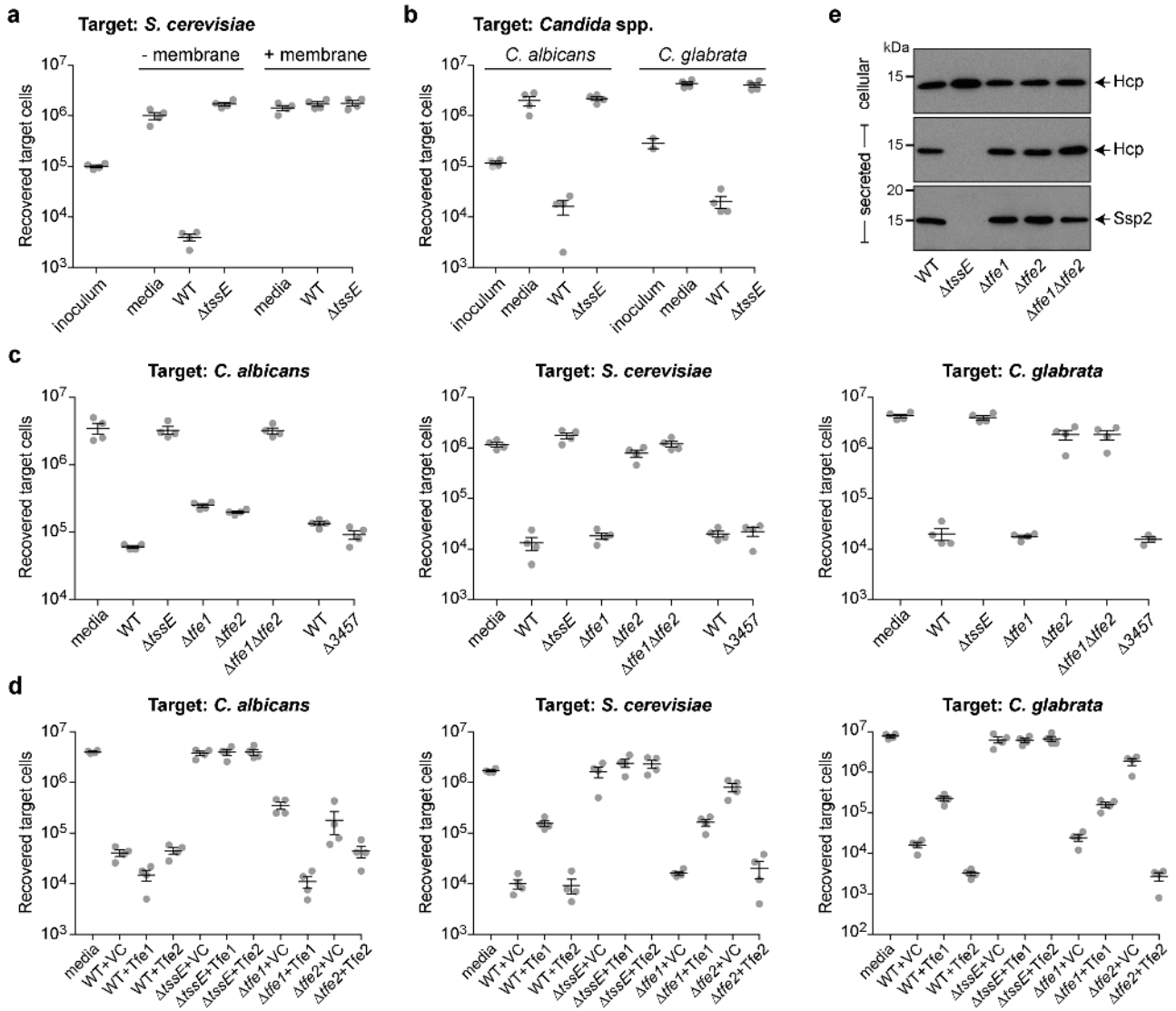


Figure 1. Cross-kingdom targeting by the Type VI secretion system of *S. marcescens* depends on the anti-fungal effectors Tfe1 and Tfe2. (a) Number of recovered viable cells of *S. cerevisiae* K699 following co-culture with wild type (WT) or a T6SS-inactive mutant ($\Delta tssE$) strain of *S. marcescens* Db10 as attacker, or with sterile media alone (media), in the absence or presence of a separating membrane. (b) Recovery of *C. albicans* SC5314 and *C. glabrata* ATCC2001 following co-culture with wild type or a T6SS-inactive mutant of *S. marcescens*. (c) Recovery of *C. albicans*, left, *S. cerevisiae*, middle, and *C. glabrata*, right, following co-culture with wild type or mutant ($\Delta tssE$, $\Delta tfe1$, $\Delta tfe2$, $\Delta tfe1\Delta tfe2$ and $\Delta SMDB11_3457$) *S. marcescens*. (d) Recovery of *C. albicans*, *S. cerevisiae* and *C. glabrata* following co-culture with wild type or mutant strains of *S. marcescens* Db10 carrying either the vector control plasmid (+VC, pSUPROM), or a plasmid directing the expression of Tfe1 with the immunity protein Sip3 (+Tfe1), or Tfe2 (+Tfe2). (e) Immunoblot detection of Hcp1 and Ssp2 in cellular and secreted fractions of wild type or mutant *S. marcescens* as indicated. In parts a-d, individual data points are overlaid with the mean +/- SEM (n=4 biological replicates).

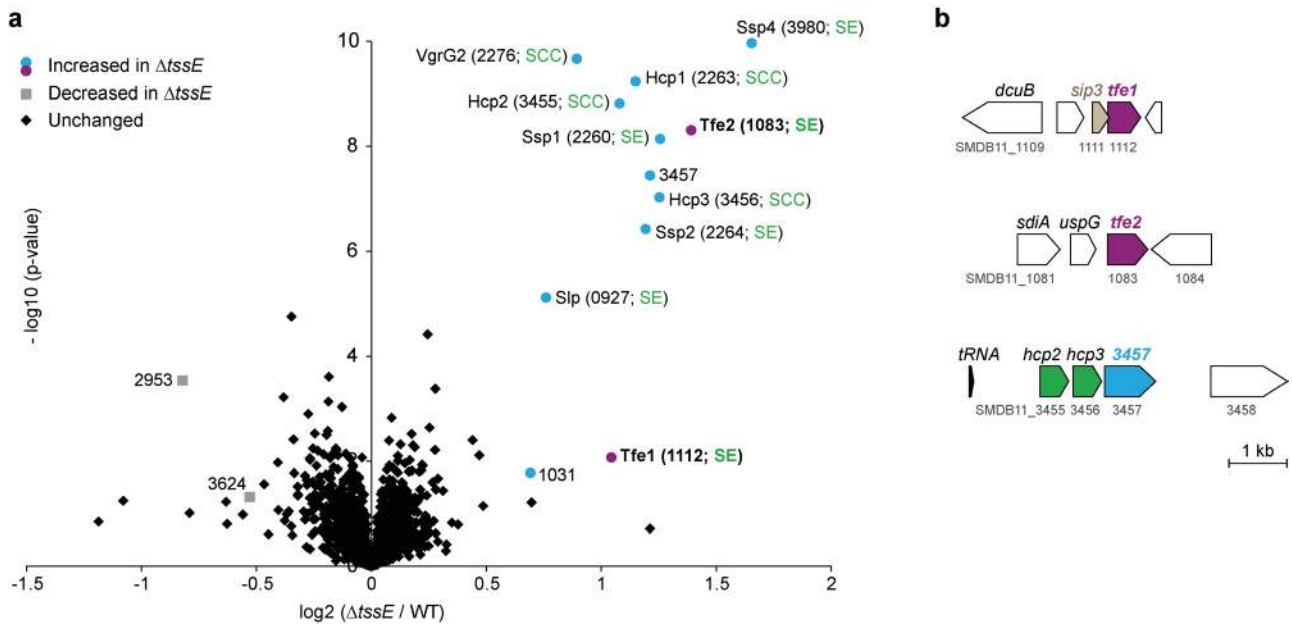


Figure 2. Quantitative cellular proteomics identifies known and new T6SS-secreted proteins. (a) Volcano plot summarising the proteomic comparison of total intracellular proteins between the wild type (WT) and a T6SS-inactive mutant ($\Delta tssE$) strain of *S. marcescens* Db10 using label-free quantitation. The \log_2 of the ratios of protein intensities between the wild type and the $\Delta tssE$ mutant are plotted against the $-\log_{10}$ of t-test p-values. Proteins significantly increased in abundance in the $\Delta tssE$ mutant compared with the wild type ($\Delta tssE/WT > 1.4$ -fold; $p < 0.05$) are depicted as circles, with magenta circles representing those secreted effectors (SE) identified as new anti-fungal effectors in this study, and blue circles representing other hits, including secreted core components (SCC) or previously identified secreted effectors. Grey squares represent proteins significantly decreased in abundance in the $\Delta tssE$ mutant compared with the wild type ($\Delta tssE/WT < -1.4$ -fold; $p < 0.05$) and black diamonds correspond to proteins without significant changes. Numbers in brackets represent genomic identifiers for the proteins (SMDB11_xxxx). (b) Schematic depiction of the genetic loci containing the *tfe1*, *tfe2* and *SMDB11_3457* genes in *S. marcescens* Db10. The *sip3* gene encodes the previously identified immunity protein for Tfe1/Ssp3.

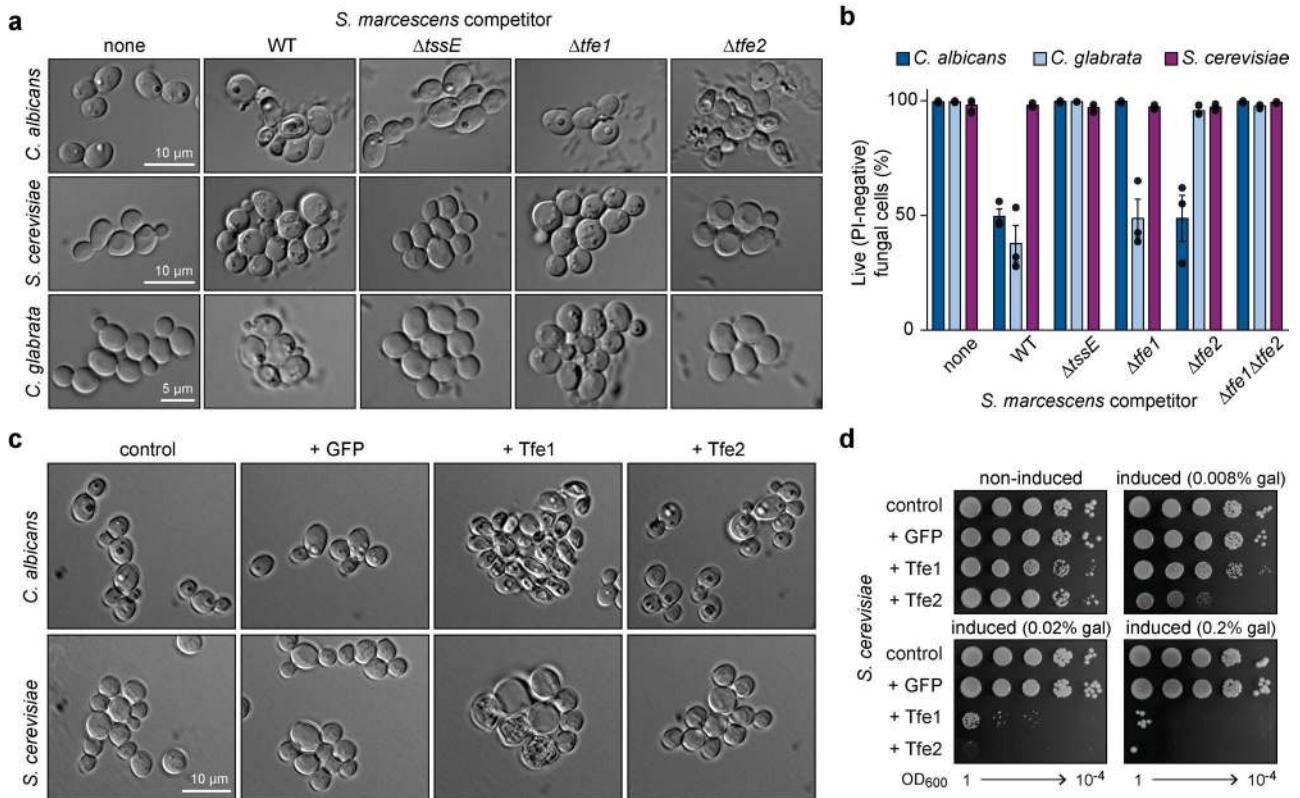


Figure 3. Tfe1 and Tfe2 are anti-fungal toxins with a species-specific impact on fungal cell integrity. (a) DIC microscopy of target strains *C. albicans* SC5314, *S. cerevisiae* K699 and *C. glabrata* ATCC2001, following co-culture with wild type or mutant ($\Delta tssE$, $\Delta tfe1$, $\Delta tfe2$, $\Delta tfe1 \Delta tfe2$) strains of *S. marcescens* Db10. ‘None’ indicates co-culture of the target with media alone. (b) Percentage of live fungal cells of *C. albicans*, *C. glabrata* and *S. cerevisiae*, following co-culture with strains of *S. marcescens*, as indicated by propidium iodide (PI) staining. Bars show mean \pm SEM (n=3 independent experiments, with individual data points shown). (c) DIC microscopy of *C. albicans* SC5314 (control) and derivatives expressing GFP, Tfe1 or Tfe2, upper panel, and *S. cerevisiae* K699 carrying the control plasmid pRB1438 or GFP-, Tfe1- or Tfe2-expression plasmids, lower panel. (d) Growth of *S. cerevisiae* K699 chromosomal integration strains harbouring the empty promoter construct (control) or constructs for expression of GFP, Tfe1 or Tfe2, on non-inducing and inducing media (gal, galactose).

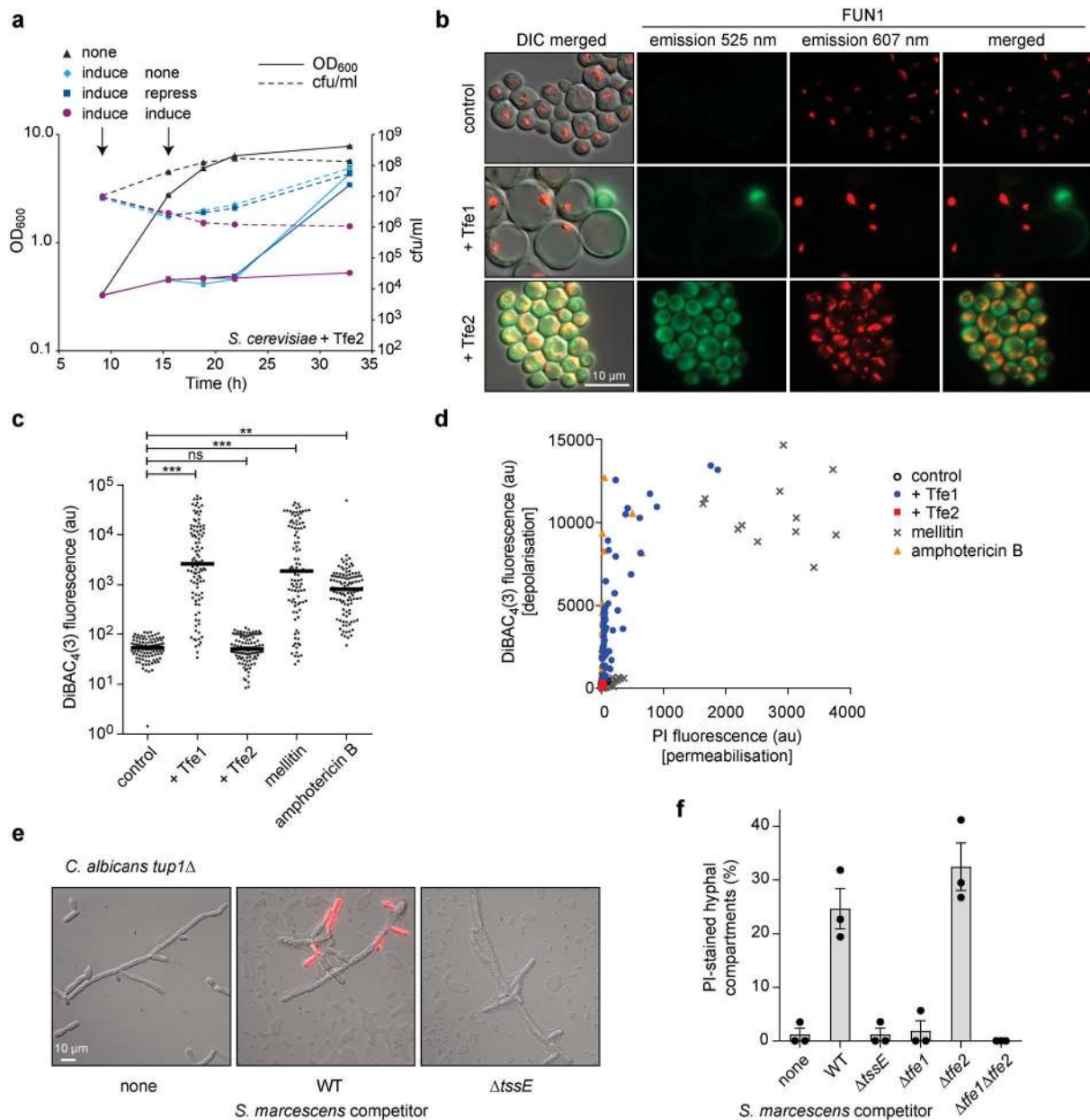


Figure 4. T6SS-mediated effector delivery disrupts fungal metabolic activity and membrane potential, and can act against hyphal cells. (a) Growth of *S. cerevisiae* expressing Tfe2 as determined by cell density (OD₆₀₀) and viable cell counts (cfu/ml). Time-course presented includes an induction period in non-inducing (none, 2% raffinose) or inducing media (induce, 2% raffinose 2% galactose), followed by either relief (none, 2% raffinose), repression (repress, 2% raffinose 2% glucose) or ongoing (induce, 2% raffinose 2% galactose) expression of Tfe2. Points show mean +/- SEM (n=3). (b) Fluorescence microscopy of FUN1-stained *S. cerevisiae* cells expressing GFP, Tfe1 or Tfe2. The single and merged green and red fluorescence channels, and their overlays on the corresponding DIC image are shown. (c) Quantification of fluorescence from *S. cerevisiae* cells expressing Tfe1 or Tfe2, following staining with the potential-sensitive dye DiBAC₄(3). Control cells were additionally treated with 100 μM mellitin (membrane depolarization through pore formation) or 3 μg/ml amphotericin B (membrane depolarization without pore formation). Points represent individual cells and bars show mean (ns, not significant;

** p<0.01; *** p<0.001; unpaired t-test). (d) Quantification of cellular DiBAC₄(3) and propidium iodide (PI) fluorescence for cells expressing Tfe1 or Tfe2, or treated with mellitin or amphotericin B. Scatter plots depict fluorescence intensity values of individual cells for both dyes (au, arbitrary units); Example microscopy images and separate scatter plots are in Supplementary Fig. 7. (a)-(d) *S. cerevisiae* strains were K699 chromosomal integration strains harbouring the empty promoter construct (control) or constructs for galactose-inducible expression of GFP, Tfe1 or Tfe2. (e) Representative images and (f) quantification of PI staining of hyphae of the constitutively filamentous *tup1Δ* mutant of *C. albicans*, following co-culture with the strains of *S. marcescens* Db10 indicated (none, media only; WT, wild type). Bars show mean +/- SEM (n=3 independent experiments, individual data points shown).

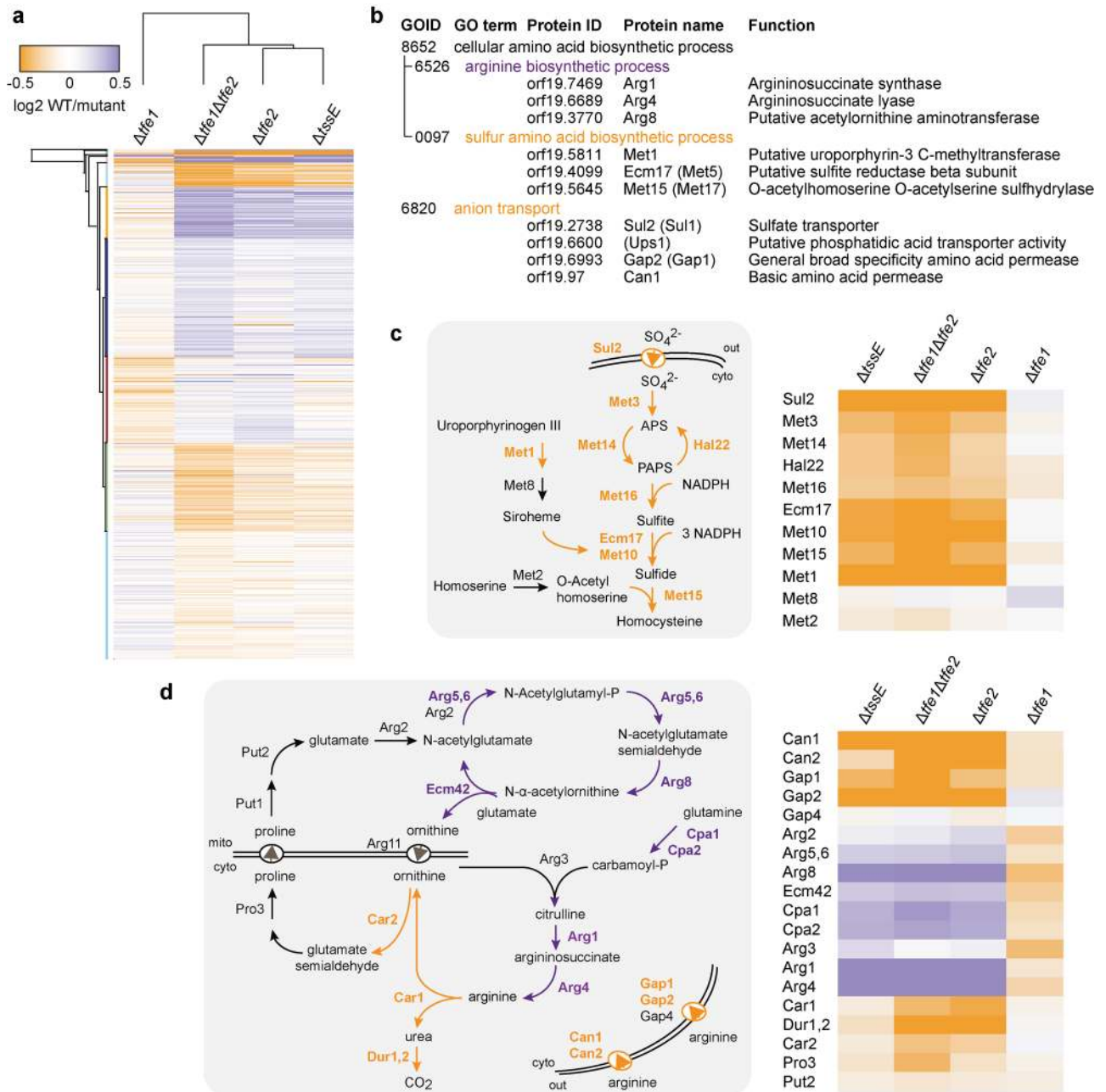


Figure 5. ‘In competition’ quantitative proteomics reveals interference of Tfe2 with fungal nutrient uptake and metabolism. (a) Heat map showing hierarchical clustering of the differential proteome of *C. albicans* SC5314 following co-culture with wild type *S. marcescens* Db10 compared with mutant ($\Delta tssE$, $\Delta tfe1$, $\Delta tfe2$ and $\Delta tfe1\Delta tfe2$) strains of Db10. All proteins with significant ANOVA scores ($p < 0.05$) are included and the full cluster analysis with gene identifiers is available as Supplementary Data 3. (b) GO terms significantly enriched ($p < 0.05$) in the set of *C. albicans* SC5314 proteins identified as significantly responsive to Tfe2 (Supplementary Table 1). Where different, the protein name in *S. cerevisiae* is given in brackets. (c,d) Schematic illustration (left panels) and corresponding heat-maps of the pathway-associated proteins (right panels) of the sulfate assimilation and arginine biosynthesis pathways in fungal cells. Proteins increased in abundance following co-culture with wild type *S. marcescens* as compared with the mutant strains indicated are shown in purple, and proteins decreased are shown in orange.

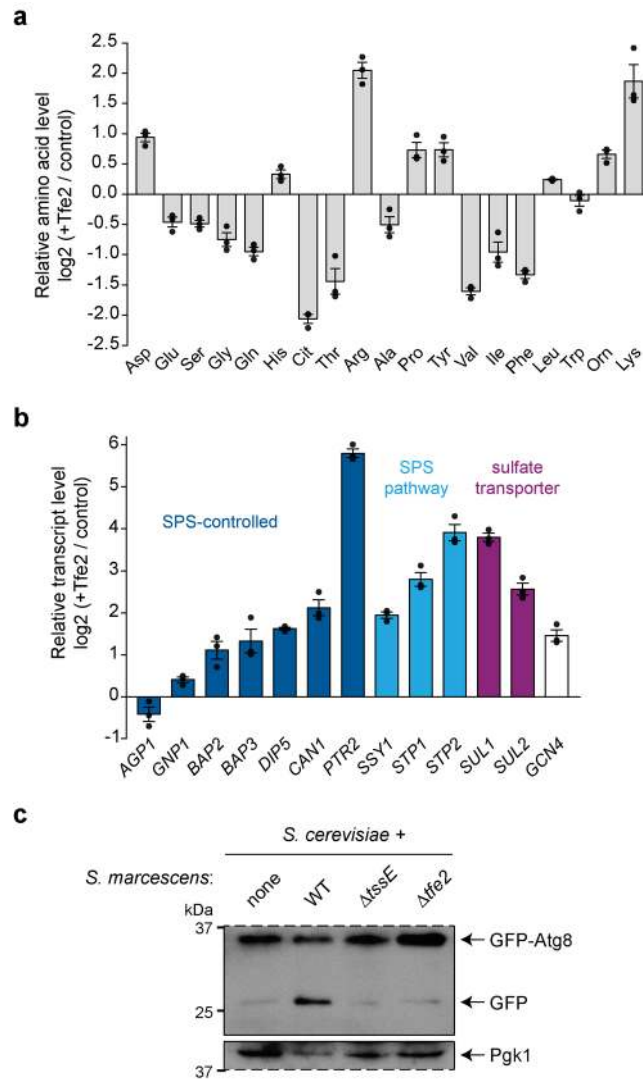


Figure 6. Tfe2 alters the cellular amino acid pool and induces autophagy in fungal cells. (a) Relative levels of total intracellular amino acids in *S. cerevisiae* K699 expressing plasmid-borne Tfe2 (+Tfe2) compared with the vector control (Cit, citrulline; Orn, ornithine). Bars show log₂ of the mean \pm SEM (n=3 biological replicates), with individual data points shown. (b) Differential expression analysis of genes involved in nutrient sensing and starvation in *S. cerevisiae* expressing Tfe2 relative to the vector control. qRT-PCR analysis was performed on transcripts of genes for amino acid permease and dipeptide transporters that are under the control of the amino acid sensor complex SPS (*AGP1*, *GNP1*, *BAP2*, *BAP3*, *DIP5*, *CAN1*, *PTR2*), the SPS sensor component (*SSY1*), the SPS-activated transcriptional regulators (*STP1*, *STP2*), the sulfate transporter (*SUL1*, *SUL2*) and the general amino acid control response regulator (*GCN4*). Bars show log₂ of the mean relative transcript abundance \pm SEM (n=3 biological replicates). (c) Immunoblot detection of GFP-Atg8 processing in *S. cerevisiae* K699 following co-culture with wild type (WT) or mutant ($\Delta tssE$ and $\Delta tfe2$) strains of *S. marcescens* Db10 using anti-GFP antibody. Yeast cells carry the reporter plasmid GFP-ATG8(416) directing expression of GFP-Atg8 from the endogenous Atg8 promoter. GFP-Atg8 has a MW of 41 kDa and cleaved GFP is 27 kDa. Pgk1 was used as control cellular protein and dashed line indicates where the blot membrane was cut to allow detection with the two different antibodies.